ACS APPLIED ENERGY MATERIALS

Letter

Over 6% Efficient Cu(In,Ga)Se2 Solar Cell Screen-Printed from Oxides on FTO

Viviana Sousa, Bruna F. Gonçalves, Yitzchak S. Rosen, Jose Virtuoso, Pedro Anacleto, M. Fátima Cerqueira, Evgeny Modin, Pedro Alpuim, Oleg I. Lebedev, Shlomo Magdassi, Sascha Sadewasser, and Yury V. Kolen'ko

ACS Appl. Energy Mater., **Just Accepted Manuscript** • DOI: 10.1021/acsaem.9b01999 • Publication Date (Web): 31 Mar 2020

Just Accepted

is published by the American Chemical Society. 1155 Sixteenth Street N.W., Washington, DC 20036

Over 6% Efficient $Cu(In,Ga)Se_2$ Solar Cell Screen-Printed from Oxides on FTO

Viviana Sousa,[a] Bruna F. Gonçalves,[a,b] Yitzchak S. Rosen,[c] José Virtuoso,[a] Pedro Anacleto[a], M. Fátima Cerqueira,[a,b] Evgeny Modin,[d] Pedro Alpuim,[a,b] Oleg I. Lebedev,[e] Shlomo Magdassi,[c] Sascha Sadewasser,[a] and Yury V. Kolen'ko[,a]*

[a] International Iberian Nanotechnology Laboratory, Braga 4715-330, Portugal

[b] Center of Physics, University of Minho, Braga 4710-057, Portugal

[c] Casali Center of Applied Chemistry, Institute of Chemistry, The Hebrew University of Jerusalem, Jerusalem 91904, Israel

[d] CIC nanoGUNE, Donostia, San Sebastian 20018, Spain

[e] Laboratoire CRISMAT, UMR 6508, CNRS-ENSICAEN, Caen 14050, France

AUTHOR INFORMATION

Corresponding Author

*yury.kolenko@inl.int

KEYWORDS: CIGSe, photovoltaics, screen-printing, ink formulation, oxides nanoparticles, microstructure.

ABSTRACT.

A new approach to fabricate copper, indium, gallium diselenide (CIGSe) solar cells on conductive fluorine-doped tin oxide (FTO) reached an efficiency of over six per cent for champion photovoltaic device. Commercial oxide nanoparticles are formulated into high-quality screen printable ink based on ethyl cellulose solution in terpineol. The high homogeneity and good adhesion properties of the oxide ink play an important role in obtaining dense and highly crystalline photoabsorber layers. This finding reveals that solution-based screen printing from readily available oxide precursors provides an interesting cost-effective alternative to current vacuum- and energy-demanding processes of the CIGSe solar cell fabrication.

TOC GRAPHICS

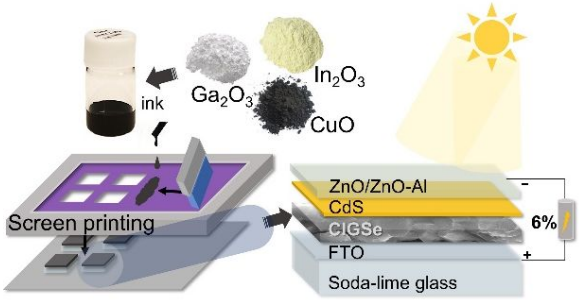

Solar cells are one of the most widely spread zero-emission energy generation technologies, which nowadays strongly rely on the first-generation silicon photovoltaics (PVs). Silicon PV is, however, somewhat hampered by the significant energy demand required to produce ca. 100 μm-thick layer of high-purity silicon.[1–3] An interesting alternative to silicon PV is offered by second generation thin-film PVs based on copper, indium, gallium diselenide (CIGSe) material with chalcopyrite structure, and the champion power conversion efficiencies for CIGSe solar cells have recently reached 23.35%.[4] CIGSe is a direct band gap p-type semiconductor with high optical absorption coefficient, which advantageously enables decreasing the thickness of the photoabsorber layer of the respective solar cell down to a few μm (theoretically down to 0.5 μm, in reality down to 1–2 μm).[1] Additionally, the resultant CIGSe PV devices are very reliable, showing degradation of only ca. 0.5% per year.

The most efficient CIGSe PV devices are currently fabricated either by co-evaporation or by sputtering, followed by a selenization step. Both depositions are expensive fabrication techniques based on vacuum processing. Interestingly, industrially compatible solution-based coating technologies, such as screen printing, inkjet printing,

spray coating, doctor blade coating, slot-die coating, or roll-to-roll processing, represent viable methods for reducing the energy demand of the CIGSe fabrication.[5] Motivated by the recent report of, in part, solution-processed $Cu(In,Ga)(S,Se)_2$ solar cells with 17.17% efficiency,[6] we became interested in developing a facile screen-printing approach to CIGSe solar cells using commercially available copper(II) oxide (CuO), indium(III) oxide (In_2O_3), and gallium(III) oxide (Ga_2O_3) as the key constitute starting materials.

We selected the screen printing process because this deposition method is feasible for large scale production, and is already widely employed in the PV industry for forming busbars with silver past. Specifically, screen-printing technology consists of a screen with a pre-patterned mesh of specific size, where the ink is forced to pass through the mesh towards the substrate, with the help of a squeegee in the direction of the substrate.[7] This technique produces μm-thick films, perfectly fitting the aforementioned required thickness of CIGSe solar cells. By using the appropriate mesh size while printing relatively viscous low volatility ink,[7] high-quality photoabsorber layers can be fabricated on a large substrate area, which is crucial for advancing printable CIGSe PVs.

So far, most of the reported efforts have focused on using inks based on $Cu(In,Ga)Se_2$ nanoparticles or metallic precursors for solution-processed CIGSe solar cells, while only few reports are available for oxide-based inks (Table S1).[8–12] Hence, we decided to leverage oxide precursors, since they are easy to synthesize and can even sometimes be harvested directly from the earth's crust,[10] and are therefore commercially readily available. In the scarce reports of metal oxides as precursors for screen printing ink formulation,[8–10] typically an intermediate thermal annealing step has to be used to reduce the pristine oxides into metals, followed by the gas transport selenization step to obtain the desired CIGSe phase. In this work, we present a robust and efficient screen-printing approach towards fabricating CIGSe PVs, which offers the practical advantage of omitting the reduction step. We also demonstrate the utility of this approach for the fabrication of CIGSe solar cells with the efficiency of over six per cent for champion PV device.

The initial point of our methodology was the formulation of high-quality oxides-based ink for screen printing. For this purpose, we subjected the selected stoichiometric mixture of commercial Cu(II), In(III), and Ga(III) oxides to wet bead milling in the presence

of di(propylene glycol) methyl ether and oleic acid. After this step, the resultant wet paste was dispersed in terpineol containing dissolved ethyl cellulose. The ethyl cellulose acts both as a rheological agent to enable high viscosity of the oxide ink, and as a binder to improve adhesion of the printed pattern to the substrate.[13] The ink was optimized to obtain a good stability, dispersion, wettability, and uniformity of the screen-printed pattern on the substrate (Figures S1–S5 in the Supporting Information (SI)). After successful screen printing of two layers of the as-formulated oxide ink on the conductive fluorine-doped tin oxide (FTO) substrate of $2.5 \times 2.5\ cm^2$, the obtained film was calcined at 400 ºC to remove carbon-based residues and subjected to rapid selenization at 550 ºC under 5%H_2/Ar flow. A detailed description of the ink formulation and properties, screen-printing parameters, calcination, selenization and adhesion of CIGSe to FTO substrate is presented in the SI.

We first investigated the phase composition of the resultant film by powder X-ray diffraction (XRD). According to the results presented in Figure 1a, the as-obtained sample is a phase mixture of FTO substrate and tetragonal CIGSe with the chalcopyrite structure.[9,14,15] Furthermore, the phase analysis demonstrates no evidence for presence

of oxides or other phases, suggesting that the metal oxides react with the selenium vapor under diluted hydrogen atmosphere forming CIGSe, $2CuO + In_2O_3 + Ga_2O_3 + 4Se + 8H_2 = 2Cu(In,Ga)Se_2 + 8H_2O$. The convenience of this synthetic protocol is that the conversion of the oxides into crystalline CIGSe is accomplished in a single step under reductive atmosphere of H_2.

We further analyzed the local structure of the as-fabricated film by Raman spectroscopy (Figure 1b), and the results are consistent with those of the XRD. A major sharp peak at 173 cm^{-1} with full width at half maximum (FWHM) of 11 cm^{-1} corresponds to the A_1 vibrational mode of CIGSe.[16,17] The broader peaks at 120 and 218 cm^{-1} are in good agreement with the B_1 and B_2/E modes of CIGSe, respectively.[17,18] Interestingly, we observed a shoulder peak at 188 cm^{-1}, which is not associated with any Cu–In–Ga–Se phases. Hence, the detected band is likely due to A_{1g} mode of $SnSe_2$ compound,[16] suggesting alloying of Sn from the FTO into the CIGSe layer (*vide infra*).

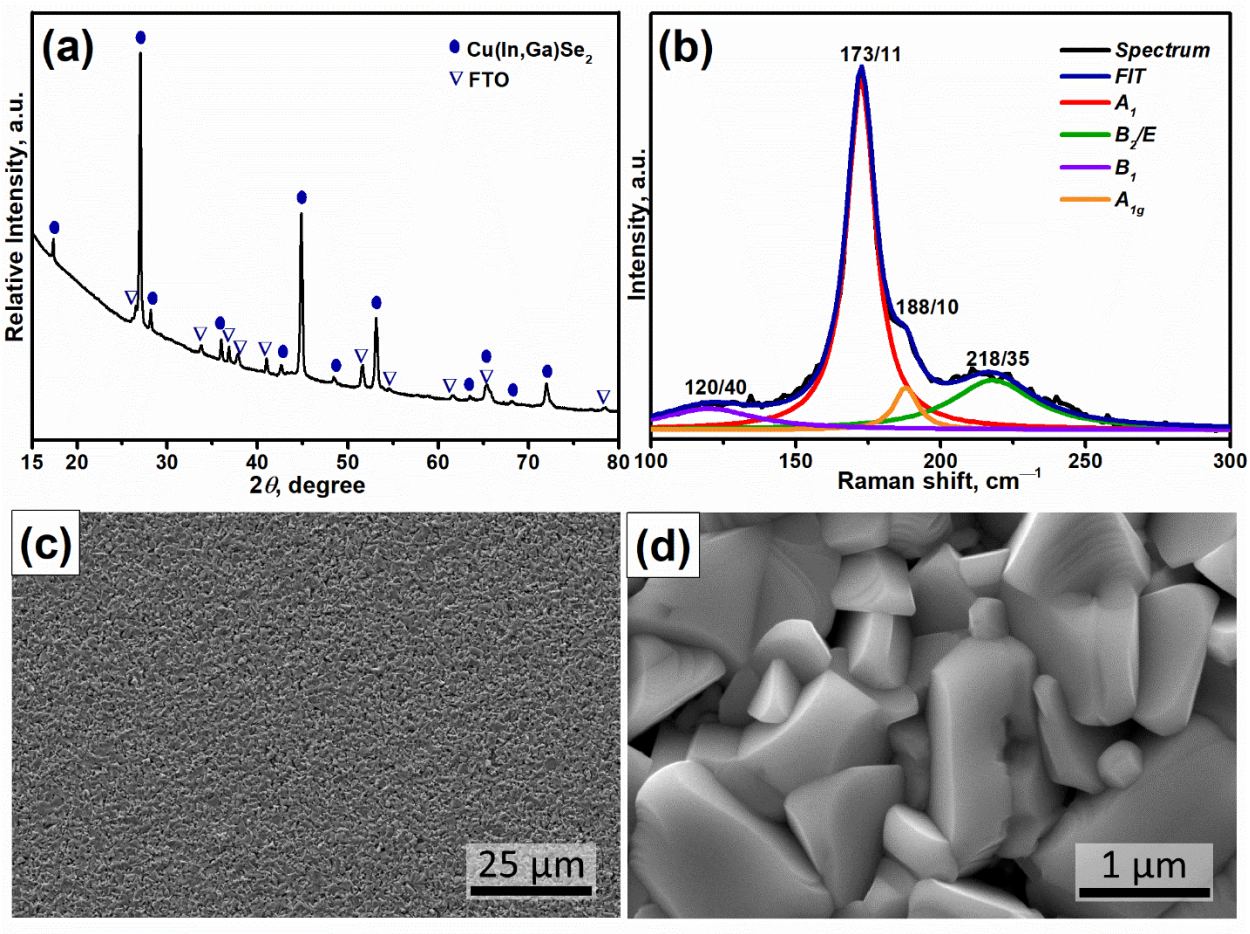

Figure 1. (a) XRD pattern of the CIGSe photoabsorber layer on FTO substrate. Ovals and triangles correspond to the positions of the most intense Bragg reflections expected for CIGSe (ICDD No. 01-083-3357, tetragonal, I–42d) and FTO, respectively. (b) Lorentzian fit (blue) of the experimental Raman data (black) for the CIGSe photoabsorber layer. The position/FWHM (in cm^{-1}) is provided for each component. Top surface low (c) and high (d) magnification SEM images of the as-fabricated CIGSe film.

We next studied the morphology, chemical composition, and stoichiometry of the obtained CIGSe photoabsorber layer by scanning electron microscopy (SEM) in conjunction with energy dispersive X-ray spectroscopy (EDX). Figures 1c,d show the overall top-view morphology of the resultant photoabsorber deposited on FTO. CIGSe

across the film exhibits a uniform and reasonably dense appearance of μm-sized crystals, indicating significant grain growth of the CIGSe phase during gas transport selenization. Accordingly, the surface of the photoabsorber layer is quite rough, which is a result of random orientation of the inter-grown CIGSe crystals, as seen in Figure 1d. The EDX analysis shows that the CIGSe phase is depleted in Ga and In in comparison to the initial oxide ratio Cu / (In + Ga) of 0.8 and Ga / (In + Ga) of 0.3, exhibiting after selenization the ratio Cu / (In + Ga) of 1.0 and Ga / (In + Ga) of 0.23.

The obtained CIGSe film which was uniformly deposited over FTO via screen printing followed by selenization, was further evaluated in terms of optical properties using ultra-violet, visible, and near infra-red spectroscopy (UV–Vis–NIR). The UV–Vis–NIR spectrum (Figure S6), shows that the as-fabricated CIGSe film absorbs strongly through the visible and into the near-infrared region. To calculate the direct bandgap (E_g), the following equation was used: $E_g = h \times c/\lambda$, where h is Planck's constant, c is the speed of light, and λ is the absorption cutoff wavelength on the absorption edge, obtained from the absorption spectra.[19] The optical absorption gap/edge of the resultant CIGSe layer

was estimated to be 1.04 eV, which is slightly lower than the optimal values (1.1–1.14 eV) reported previously for bulk CIGSe chalcopyrite.[2,5]

The above characterization evidences that screen printing of oxide-based ink followed by gas transport selenization enables the formation of semiconducting CIGSe photoabsorber layer. Accordingly, we moved forward with the fabrication of CIGSe PV devices, as summarized in the SI. Briefly, to create a heterojunction, we first deposited a 70 nm buffer layer of n-type cadmium sulfide (CdS) using chemical bath deposition on top of the freshly fabricated ≈2 μm-thick CIGSe film on FTO glass. Next, a 50 nm resistive intrinsic zinc oxide (i-ZnO) was sputtered on FTO/CIGSe/CdS, followed by sputtering 200 nm transparent conducting window layer of aluminum-doped zinc oxide (ZnO:Al). This fabrication procedure enables a reliable process for fabrication of FTO/CIGSe/CdS/i-ZnO/ZnO:Al solar cells. The top morphology of the device is shown in Figure S7. Although the overall surface of the PV device is somewhat irregular due to the roughness of the original CIGSe layer (Figure 1c, d), the top transparent ZnO:Al and the resistive i-ZnO layers were homogeneously deposited onto the surface of FTO/CIGSe/CdS.

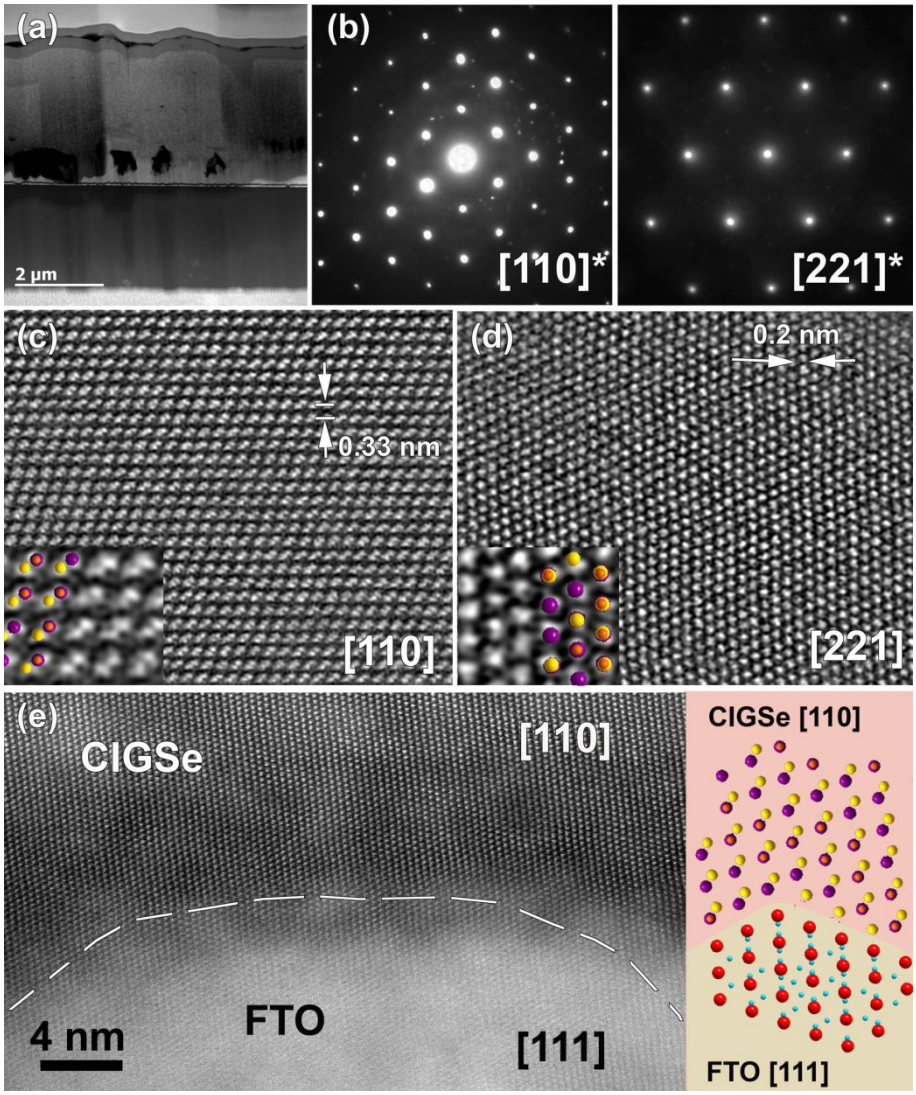

Figure 2. (a) Cross-sectional HAADF–STEM image of the fabricated FTO/CIGSe/CdS/i-ZnO/ZnO:Al PV device. (b) [110] and [221] SAED patterns of selected CIGSe grains and (c, d) the corresponding high-resolution HAADF–STEM images along [110] and [221] zone axes. Enlargement images with overlaid structural model are given as insert (purple atoms: In/Ga, orange: Cu and yellow: Se). (e) High-resolution HAADF–STEM image of the interface between FTO and CIGSe, demonstrating nearly epitaxial growth of [110] CIGSe on [111] FTO together with the corresponding structural model (red: Sn, blue: O).

We further conducted cross-sectional investigation of the resultant PV device by means of transmission electron microscopy (TEM). For this purpose, a focused ion beam

TEM specimen preparation was employed for cross-sectioning of the film. The representative SEM images of the obtained lamella are shown in Figure S8, while Figure 2 summarizes the high angle annular dark field scanning TEM (HAADF–STEM) observation of the lamella together with selected area electron diffraction (SAED) studies. A multilayered microstructure of the PV device is confirmed by STEM observations (Figure 2a, S9). The presence voids, which are microstructural defects at the interface between FTO substrate and CIGSe layer, can be clearly seen (Figures 2a, S8, S9), in agreement with the literature.[20] The grains of the photoabsorber CIGSe layer itself are highly crystalline and structurally defect-free, as seen in the HAADF-STEM images and the corresponding SAED patterns (Figures 2b–d). Regardless of the aforementioned voids observed at the FTO/CIGSe interface, our HAADF–STEM imaging of the interface reveals nearly epitaxial growth of the CIGSe on top of the FTO substrate (Figure 2e), suggesting the existence of good interfacial/electrical contact between the photoabsorber and back contact.

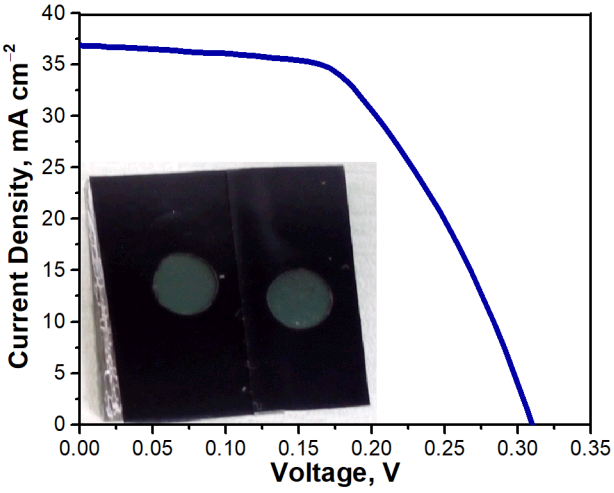

Figure 3. *J–V* curve of the as-fabricated champion PV device reaching 6.1% efficiency, J_{sc} of 36.8 mA/cm^{-2}, V_{oc} of 0.31 V and *FF* of 53.8% (inset picture of PV device).

After fabrication and structural characterization of the PV devices, we assessed the photovoltaic performance of the FTO/CIGSe/CdS/i-ZnO/ZnO:Al solar cells masked with an active area of 0.28 cm^2 under a solar simulator with source illumination of 100 mW cm^{-2} (Figure 3). Totally ten PV cells have been fabricated and an average efficiency of 2.9 ± 1.6 % was measured (Table S2). The champion solar cell exhibits a short-circuit current density (J_{sc}) of 36.8 mA cm^{-2}, open-circuit voltage (V_{oc}) of 0.31 V, and fill factor (FF) of 53.8%. These values lead to ca. 6.1% efficiency of the resultant champion FTO/CIGSe/CdS/i-ZnO/ZnO:Al solar cell (Figure 4a). Importantly, the efficiency

measurements after two months gave nearly identical performance as in the case of just fabricated PV devices, marking the durability of the as-fabricated CIGSe solar cells (Figure 4b). The high short-circuit current of the campion device can be correlated with the low bandgap (1.04 eV) obtained for the CIGSe photoabsorber layer. As for V_{oc}, a significantly reduced value, comparing with high performance CIGSe[21] was measured, which we attribute to recombination losses and to the low bandgap. Regarding FF, we can assume that the series resistance is dominating the losses on this parameter, which could be related to interface problems between the back contact and the photoabsorber, such as the confirmed presence of voids.

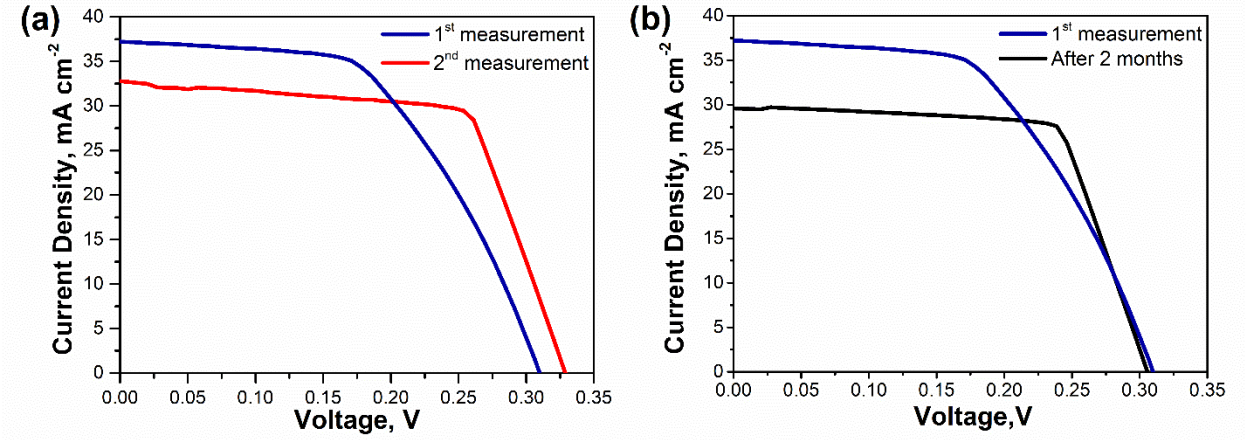

Figure 4. (a) J–V curves of champion PV cell recorded on the same day. (b) J–V curves of champion PV cell measured on the day of fabrication and after two months.

To better understand the arrangement of solar cell layers, the cross-sectional chemical composition and the distribution of all elements through the PV device was analyzed by EDX mapping in STEM mode. Figure 5 shows STEM−EDX mapping of the representative FTO/CIGSe/CdS/i-ZnO/ZnO:Al PV device. Starting from the top of the PV device, the presence of In is detected in CdS layer, resulting in CdS + In composition of the resultant buffer layer responsible for the heterojunction. Furthermore, the distribution of Ga within the CIGSe layer was found to be markedly inhomogeneous, showing the existence of segregated Ga–O inclusions within the photoabsorber layer (Figures 5 and S10). Since we used commercial CuO and In_2O_3 nanopowders for ink formulation and polycrystalline Ga_2O_3 as a precursor (Ga_2O_3 nanopowder is not commercially available), it seems that even after wet bead milling, the size of Ga_2O_3 is not reduced down to nanometer size, thus resulting in the existence of not fully reacted Ga–O segregations in the CIGSe layer due to the low reactivity of the relatively large Ga_2O_3 particles. Accordingly, the lack of a sufficient amount of Ga in the CIGSe layer could contribute to its reduced band gap value and accordingly low V_{oc}.[22] In addition, the presence of the

Ga–O phase inclusions in the CIGSe layer can be considered as recombination centers for holes and electrons, thus lowering the overall PV device performance.

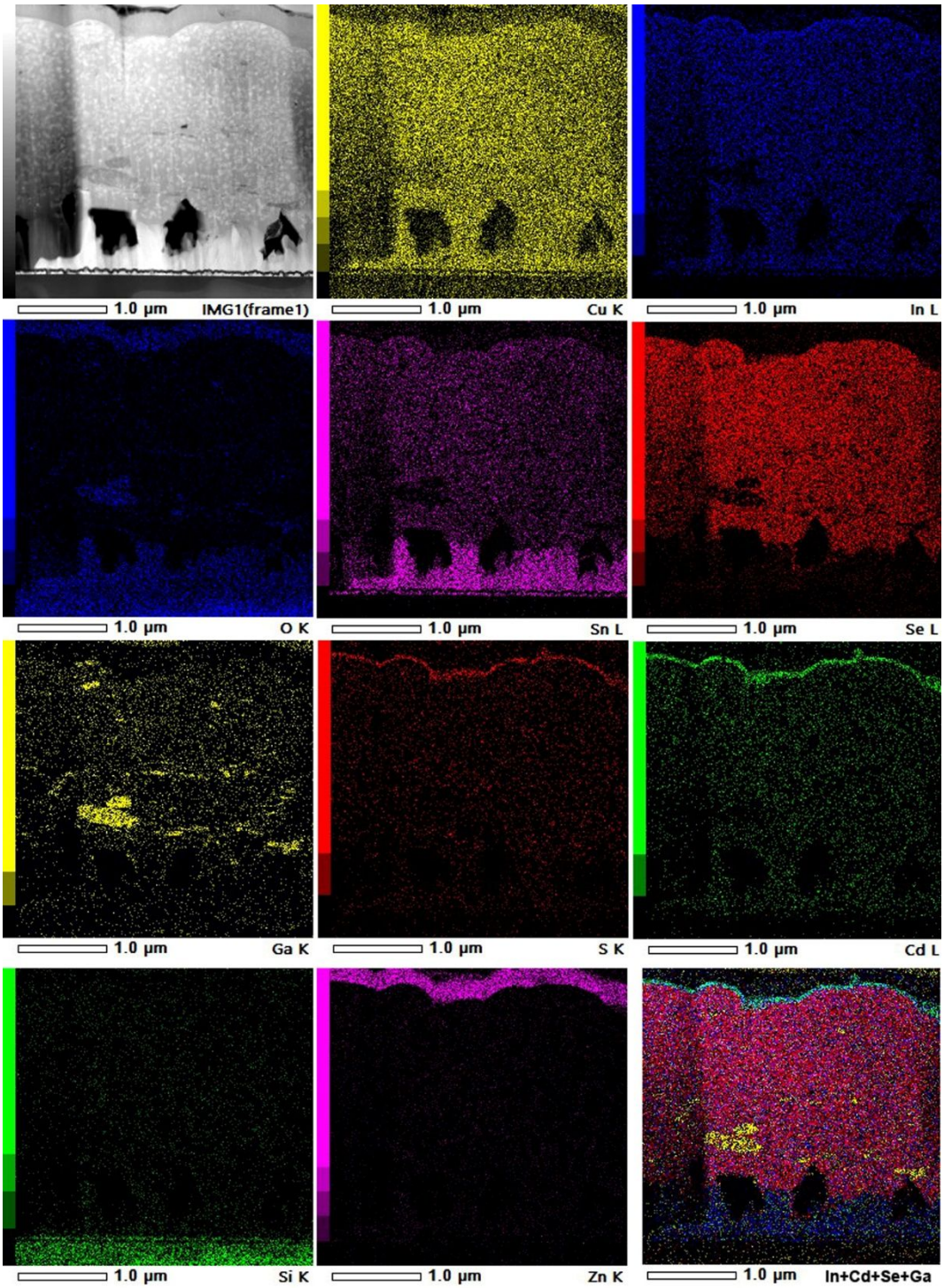

Figure 5. Cross-section HAADF−STEM image of the FTO/CIGSe/CdS/i-ZnO/ ZnO:Al PV device, together with the simultaneously collected EDX maps of Cu, In, O, Sn, Se, Ga, S, Cd, Si, Zn, as well as In, Cd, Se, Ga mixture.

Interestingly, from Figure 5, the migration of tin from FTO into the CIGSe layer is clearly observed, resulting in an intermixing of Sn, Cu, and In at the FTO/CIGSe interface. This migration most likely occurs during gas transport selenization process and leads to formation of the aforementioned void defects at the interface between the photoabsorber and back contact.[20] Such modification of the FTO back contact possibly gives rise to rear interface recombination, hence, lowering V_{oc}, and accordingly, device performance.[10] The interface recombination also gives rise to moderate FF as a result of high series resistance, suggesting that further improvements of the absorber/back junction should be conducted to avoid recombination losses, as well as associated high series resistance.[10,12,23,24]

Notably, soda–lime glass (SLG) with ≈0.5 μm layer of Mo is known to be a good substrate/back contact for CIGSe solar cells, and we initially employed this Mo/SLG type of substrate in our screen-printing-assisted fabrication procedure. However, we experimentally found that Mo cannot resist gas transport selenization at 550 ºC for 30 min

under 5%H_2/Ar flow, as it entirely transforms into $MoSe_2$, as confirmed by XRD. This transformation resulted in the strong peeling of the resultant CIGSe layer from the SLG substrate (Figure S11). Importantly, by switching the back contact to FTO, we demonstrated that a reliable CIGSe solar cells can be fabricated.

In conclusion, we describe a robust printing-based method for the fabrication of CIGSe solar cells. Oxide ink formulation, screen-printing, and calcination followed by gas transport selenization provide ≈2 μm thick polycrystalline CIGSe photoabsorber layer grown on top of FTO/glass substrates. One of the key points of this approach is that the oxide reduction and selenization are conducted in a single step. After depositing the buffer and window layers, several FTO/CIGSe/CdS/i-ZnO/ZnO:Al solar cell devices were completed and the champion one exhibited 6.1% efficiency. To the best of our knowledge, this is the topmost performance for CIGSe solar cell fabricated from oxide precursors on FTO (Table S1).[4-6,8,10,12,19,25–30] We believe that the demonstrated feasibility of our screen printing approach from oxides can inspire new research efforts for fabricating fully-printed CIGSe PV in a cost-effective manner.

Our investigation further showed that the PV properties are strongly influenced by interface recombination due to compositional and microstructural variation within the PV device, suggesting that improvements should be done to enhance the device performance by optimizing the photoabsorber/back contact interface and the chemical composition of the CIGSe phase. This is the subject of our ongoing research.

ASSOCIATED CONTENT

The supporting information (SI) is available free of charge on the ACS Publications website. Materials and methods and additional optical microscopy, electron microscopy and visualization data (PDF).

CORRESPONDING AUTHOR

*yury.kolenko@inl.int

Notes

The authors declare no competing financial interest.

ACKNOWLEDGEMENT

We thank the members of the Nanochemistry Research Group at INL for valuable discussions. This work was supported by ERDF COMPETE 2020 and Portuguese FCT funds under the PrintPV project (PTDC/CTM-ENE/5387/2014, Grant Agreement No. 016663). B.F.G. is grateful to the FCT for the SFRH/BD/121780/2016 grant.

REFERENCES

(1) Coughlan, C.; Ibáñez, M.; Dobrozhan, O.; Singh, A.; Cabot, A.; Ryan, K. M. Compound Copper Chalcogenide Nanocrystals. *Chem. Rev.* **2017**, *117*, 5865–6109.

(2) Ramanujam, J.; Singh, U. P.; Tomassini, M.; Barreau, N.; Steijvers, H.; Berkumd, J. van; Vroon, Z.; Zeman, M.; Zimmermann, U.; Cunha, A. F. da; Edoff, M.; Nishiwaki, S.; Romanyuk, Y. E.; Bilger, G.; Tiwari, A. N.; Bjorkman, C. P.; Spiering,

S.; Tiwari, A. N.; Torndahl, T.; Cirlin, G. E. Copper Indium Gallium Selenide Based Solar Cells – a Review. *Energy Environ. Sci.* **2017**, *10*, 1306–1319.

(3) Terheiden, B.; Ballmann, T.; Horbelt, R.; Schiele, Y.; Seren, S.; Ebser, J.; Hahn, G.; Mertens, V.; Koentopp, M. B.; Scherff, M.; Müller, J. W.; Holman, Z. C.; Descoeudres, A.; Wolf, S. De; Nicolas, S. M. de; Geissbuehler, J.; Ballif, C.; Weber, B.; Saint-Cast, P.; Rauer, M.; Schmiga, C.; Glunz, S. W.; Morrison, D. J.; Devenport, S.; Antonelli, D.; Busto, C.; Grasso, F.; Ferrazza, F.; Tonelli, E.; Oswald, W. Manufacturing 100-µm-Thick Silicon Solar Cells with Efficiencies Greater than 20% in a Pilot Production Line. *Phys. Status Solidi A* **2015**, *212*, 13–24.

(4) Solar Frontier. Solar Frontier Achieves World Record Thin-Film Solar Cell Efficiency of 23.35%.

(5) Roux, F.; Amtablian, S.; Anton, M.; Besnard, G.; Bilhaut, L.; Bommersbach, P.; Braillon, J.; Cayron, C.; Disdier, A.; Fournier, H.; Garnier, J.; Jannaud, A.; Jouhannaud, J.; Kaminski, A.; Karst, N.; Noël, S.; Perraud, S.; Poncelet, O.; Raccurt, O.; Rapisarda, D.; Ricaud, A.; Rouchon, D.; Roumanie, M.; Rouviere, E.;

Sicardy, O.; Sonier, F.; Tarasov, K.; Tardif, F.; Tomassini, M.; Villanova, J. Chalcopyrite Thin-Film Solar Cells by Industry-Compatible Ink-Based Process. *Sol. Energy Mater. Sol. Cells* **2013**, *115*, 86–92.

(6) Eeles, A.; Arnou, P.; Bowers, J. W.; Walls, J. M.; Whitelegg, S.; Kirkham, P.; Allen, C.; Stubbs, S.; Liu, Z.; Masala, O.; Newman, C.; Pickett, N. High-Efficiency Nanoparticle Solution-Processed $Cu(In,Ga)(S,Se)_2$ Solar Cells. *IEEE J. Photovoltaics* **2018**, *8*, 288–292.

(7) Krebs, F. C. Fabrication and Processing of Polymer Solar Cells: A Review of Printing and Coating Techniques. *Sol. Energy Mater. Sol. Cells* **2009**, *93*, 394–412.

(8) Kapur, V. K.; Bansal, A.; Le, P.; Asensio, O. I. Non-Vacuum Processing of $CuIn_{1-x}Ga_xSe_2$ Solar Cells on Rigid and Flexible Substrates Using Nanoparticle Precursor Inks. *Thin Solid Films* **2003**, *431–432*, 53–57.

(9) Lee, E.; Park, S. J.; Cho, J. W.; Gwak, J.; Oh, M. K.; Min, B. K. Nearly Carbon-Free Printable CIGS Thin Films for Solar Cell Applications. *Sol. Energy Mater. Sol. Cells* **2011**, *95*, 2928–2932.

(10) Pulgarín-Agudelo, F. A.; López-Marino, S.; Fairbrother, A.; Placidi, M.; Izquierdo-Roca, V.; Sebastián, P. J.; Ramos, F.; Pina, B.; Pérez-Rodríguez, A.; Saucedo, E. A Thermal Route to Synthesize Photovoltaic Grade $CuInSe_2$ Films from Printed CuO/In_2O_3 Nanoparticle-Based Inks under Se Atmosphere. *J. Renew. Sustain. Energy* **2013**, *5*, 053140.

(11) Kuo, H. P.; Tsai, H. A.; Huang, A. N.; Pan, W. C. CIGS Absorber Preparation by Non-Vacuum Particle-Based Screen Printing and RTA Densification. *Appl. Energy* **2016**, *164*, 1003–1011.

(12) López-García, J.; Xie, H.; Izquierdo-Roca, V.; Sylla, D.; Fontané, X.; Blanes-Guardia, M.; Ramos, F.; Espindola-Rodriguez, M.; López-Marino, S.; Saucedo, E.; Pérez-Rodriguez, A. Synthesis of $CuIn(S,Se)_2$ Quaternary Alloys by Screen Printing and Selenization-Sulfurization Sequential Steps: Development of Composition Graded Absorbers for Low Cost Photovoltaic Devices. *Mater. Chem. Phys.* **2015**, 237–243.

(13) Rosen, Y.; Marrach, R.; Gutkin, V.; Magdassi, S. Thin Copper Flakes for

Conductive Inks Prepared by Decomposition of Copper Formate and Ultrafine Wet Milling. *Adv. Mater. Technol.* **2019**, *4*, 1800426.

(14) Zhang, C.; Zhu, H.; Liang, X.; Zhou, D.; Guo, Y.; Niu, X.; Li, Z.; Chen, J.; Mai, Y. Influence of Heating Temperature of Se Effusion Cell on Cu(In,Ga)Se_2 Thin Films and Solar Cells. *Vacuum* **2017**, *141*, 89–96.

(15) Cheng, K.; Han, K.; Kuang, Z.; Jin, R.; Hu, J.; Guo, L.; Liu, Y.; Lu, Z.; Du, Z. Optimization of Post-Selenization Process of Co-Sputtered CuIn and CuGa Precursor for 11.19% Efficiency Cu(In,Ga)Se_2 Solar Cells. *J. Electron. Mater.* **2017**, *46*, 2512–2520.

(16) Yan, Y.; Guo, T.; Song, X.; Yu, Z.; Jiang, Y.; Xia, C. Cu(In,Ga)Se_2 Thin Films Annealed with $SnSe_2$ for Solar Cell Absorber Fabricated by Magnetron Sputtering. *Sol. Energy* **2017**, *155*, 601–607.

(17) Rincón, C.; Ramírez, F. J. Lattice Vibrations of $CuInSe_2$ and $CuGaSe_2$ by Raman Microspectrometry. *J. Appl. Phys.* **1992**, *72*, 4321–4324.

(18) Witte, W.; Kniese, R.; Powalla, M. Raman Investigations of Cu(In ,Ga)Se_2 Thin Films with Various Copper Contents. *Thin Solid Films* **2008**, *517*, 867–869.

(19) Chen, Q.; Dou, X.; Li, Z.; Cheng, S.; Zhuang, S. Printed Ethyl Cellulose/$CuInSe_2$ Composite Light Absorber Layer and Its Photovoltaic Effect. *J. Phys. D. Appl. Phys.* **2011**, *44*, 455401.

(20) Jiang, J.; Yu, S.; Gong, Y.; Yan, W.; Zhang, R.; Liu, S.; Huang, W.; Xin, H. 10.3 % Efficient $CuIn(S,Se)_2$ Solar Cells from DMF Molecular Solution with the Absorber Selenized under High Argon Pressure. *Sol. RRL* **2018**, *1800044*, 1–7.

(21) Kato, T.; Wu, J.; Hirai, Y.; Sugimoto, H.; Bermudez, V. Record Efficiency for Thin-Film Polycrystalline Solar Cells Up to 22.9% Achieved by Cs-Treated $Cu(In,Ga)(Se,S)_2$. *IEEE J. Photovoltaics* **2018**, *9*, 325–330.

(22) Kim, B.; Min, B. K. Strategies toward Highly Efficient CIGSe Thin-Film Solar Cells Fabricated by Sequential Process. *Sustain. Energy Fuels* **2018**, *2*, 1671–1685.

(23) Nakane, A.; Tampo, H.; Tamakoshi, M.; Fujimoto, S.; Kim, K. M.; Kim, S.; Shibata,

H.; Niki, S.; Fujiwara, H. Quantitative Determination of Optical and Recombination Losses in Thin-Film Photovoltaic Devices Based on External Quantum Efficiency Analysis. *J. Appl. Phys.* **2016**, *120*, 064505.

(24) Cui, Y.; Zhang, Z.; Du, X.; Liu, W.; Liu, S.; Deng, Y.; Huang, X.; Wang, G. Efficient Hybrid Solution Strategy to Fabricate $Cu(In,Ga)(S,Se)_2$ Solar Cells. *J. Alloys Compd.* **2017**, *696*, 884–890.

(25) Khavar, A. H. C.; Mahjoub, A. R.; Taghavinia, N. Low-Temperature Solution-Based Processing to 7.24% Efficient Superstrate $CuInS_2$ Solar Cells. *Sol. Energy* **2017**, *157*, 581–586.

(26) Mcleod, S. M.; Hages, C. J.; Carter, N. J.; Agrawal, R. Synthesis and Characterization of 15% Efficient CIGSSe Solar Cells from Nanoparticle Inks. *Prog. Photovoltaics Res. Appl.* **2015**, *23*, 1550–1556.

(27) Uhl, A. R.; Katahara, J. K.; Hillhouse, H. W. Molecular-Ink Route to 13.0% Efficient Low-Bandgap $CuIn(S,Se)_2$ and 14.7% Efficient $Cu(In,Ga)(S,Se)_2$ Solar Cells. *Energy Environ. Sci.* **2016**, *9*, 130–134.

(28) Berner, U.; Colombara, D.; Wild, J. De; Robert, E. V. C.; Schütze, M.; Hergert, F.; Valle, N.; Widenmeyer, M.; Dale, P. J. 13.3% Efficient Solution Deposited $Cu(In,Ga)Se_2$ Solar Cells Processed with Different Sodium Salt Sources. *Prog. Photovoltaics Res. Appl.* **2016**, *24*, 749–759.

(29) Todorov, T. K.; Gunawan, O.; Gokmen, T.; Mitzi, D. B. Solution-Processed $Cu(In,Ga)(S,Se)_2$ Absorber Yielding a 15.2% Efficient Solar Cell. *Prog. Photovoltaics Res. Appl.* **2013**, *21*, 82–87.

(30) Arnou, P.; Cooper, C. S.; Uličná, S.; Abbas, A.; Eeles, A.; Wright, L. D.; Malkov, A. V.; Walls, J. M.; Bowers, J. W. Solution Processing of $CuIn(S,Se)_2$ and $Cu(In,Ga)(S,Se)_2$ Thin Film Solar Cells Using Metal Chalcogenide Precursors. *Thin Solid Films* **2017**, *633*, 76–80.